

## DESIGN AND DEVELOPMENT OF SUNFLOWER INTELLIGENT INSERTION TRAY DRYER

### 向日葵智能插盘晾晒机的设计与开发

Qiang WANG <sup>1)</sup>, Xinyuan WEI <sup>1)</sup>, Keqi YAN <sup>1)</sup>, Qiyuan XUE <sup>1)</sup>, Yangcheng LV <sup>1)</sup>,  
Yaoyu Li <sup>1,2)</sup>, Wuping ZHANG <sup>1\*)</sup>, Fuzhong LI <sup>1)</sup>

<sup>1)</sup> College of Software, Shanxi Agricultural University, Taigu, Shanxi / China

<sup>2)</sup> College of Agricultural Engineering, Shanxi Agricultural University, Taigu, Shanxi / China

Tel: +8603546287093; E-mail: zwping@126.com

Corresponding author: Zhang Wuping

DOI: <https://doi.org/10.35633/inmateh-74-14>

**Keywords:** sunflower; intelligent Plug-in Tray Dryer; Agricultural Engineering; You Only Look Once version 5 (YOLOv5); Lightweight and Ground Optimized Lidar Odometry and Mapping (LeGO-LOAM)

#### ABSTRACT

In order to meet the demand for mechanisation of sunflower segmented harvesting and tray insertion for drying, an intelligent tray insertion dryer was designed and developed. The machine integrates the functions of disc picking, disc flipping, bar clipping, lifting and inserting, and uses SolidWorks for accurate mechanism design and simulation, incorporating the YOLOv5 model for efficient recognition of flower discs and the LeGO-LOAM algorithm for accurate navigation and map building. In the experiment, 81 sunflower samples were collected to analyse data on disc diameter, plant height, rod diameter and stalk diameter, and to verify the recognition accuracy of the YOLOv5 model in different directions. The results showed that the precision of disc recognition was 95.54%, accuracy was 89.94%, recall was 95.54% and F1 value was 0.89. Using the LeGO-LOAM algorithm tested at different path lengths, the root-mean-square error of the navigational build trajectory was 0.15 m, with a standard deviation of 0.10 m. This technological integration improves the operational efficiency and supports the mechanisation of sunflower insertion tray drying.

#### 摘要

为了满足向日葵分段收获和插盘晾晒的机械化需求,我们设计并开发了一款智能插盘晾晒机。该机集成了摘盘、翻盘、剪杆、升降和插盘等功能,采用 SolidWorks 进行精确的机构设计和模拟,融合了 YOLOv5 模型的高效识别花盘和 LeGO-LOAM 算法的精确导航建图。实验中,采集了 81 株向日葵样本,分析花盘直径、株高、杆径和梗径数据,并验证 YOLOv5 模型在不同方向上的识别精度。结果显示,花盘识别精度达 95.54%, 准确度为 89.94%, 召回率为 95.54%, F1 值为 0.89。利用 LeGO-LOAM 算法在不同路径长度下测试,导航建图轨迹的均方根误差为 0.15m, 标准差为 0.10m。这种技术整合提高了作业效率,为向日葵插盘晾晒机械化提供了支持。

#### INTRODUCTION

In the era of electronic information, intelligent agricultural machinery, as multifunctional equipment, is combined with automation technology to promote the development of modern agriculture (Jin *et al.*, 2021; Dhanaraju *et al.*, 2022). At present, the harvesting process of major food crops around the world has been commonly mechanised (Peng *et al.*, 2022). According to the Food and Agriculture Organization of the United Nations (FAO), the sunflower planting area in China has stabilised at around 1 million hectares in the last decade, with an annual output of between 2.4 million and 2.6 million tonnes (Moschen *et al.*, 2017). However, the mechanisation level of sunflower harvesting is still low, mainly relying on manual and limited mechanised means for sectioning and joint harvesting (Pan *et al.*, 2024).

The insertion of sunflower trays for drying can accelerate the dehydration process of flower trays and seeds, promote the full maturation of seeds, improve the appearance quality and overall cleanliness, and reduce the risk of mould caused by improper stacking. By inserting the disk directly on the stalks for drying, it not only effectively solves the shortage of drying sites, but also facilitates the efficient operation of walking threshing machines in the field, further improving the overall efficiency of field management.

Qiang WANG, M.S. Stud. Agr.; Xinyuan WEI, M.S. Stud. Eng.; Keqi YAN, M.S. Stud. Eng.; Qiyuan XUE, M.S. Stud. Agr.; Yangcheng LV, M.S. Stud. Agr.; Yaoyu Li, Ph.D.Eng.; Wuping ZHANG, Prof. Ph.D. Eng.; Fuzhong LI, Prof. Ph.D. Eng.

In this paper, an intelligent sunflower insertion tray drying machine is designed, which integrates the functions of picking, turning, cutting stems, lifting, inserting trays, etc., to meet the mechanization needs of sunflower harvesting and drying in the field environment. Traditional sunflower harvesting and drying methods usually rely heavily on manual operation or single-function harvesting equipment, which has problems such as low efficiency, high labour intensity, and unstable drying quality. At the same time, the traditional equipment usually can only complete the single task of cutting and handling, lack of insertion plate drying follow-up operation function, need to additionally configure other equipment or manual processing, thus increasing the operational complexity and cost.

To address these shortcomings, the intelligent sunflower insertion tray drying machine designed in this paper realizes the whole process automation from picking to drying through integrated design. The device combines deep learning and navigation technologies to accurately recognize the sunflower position and intelligently adjust the operation path and attitude to ensure the precise handling and consistency of each disk. Compared to traditional methods, the intelligent equipment has significant advantages in reducing labour costs and improving operational precision and efficiency, making it particularly suitable for small- and medium-scale sunflower planting sites. While controlling costs, the design can effectively improve field operation efficiency, providing a more efficient and intelligent solution for agricultural mechanization. (Dong *et al.*, 2017).

## MATERIALS AND METHODS

### Overall structure

In order to the integrity of the machine function and the intelligence of the insert tray drying work, this paper selects the idea of modular design (Li *et al.*, 2017). The functional structure of the machine body is designed first, and then the intelligent function is expanded to gradually transition from mechanisation to intelligence. It can make the structure of the machine complete and reliable, and also make the upgrading and transformation of the body more flexible, and finally complete the established function of insert tray drying.

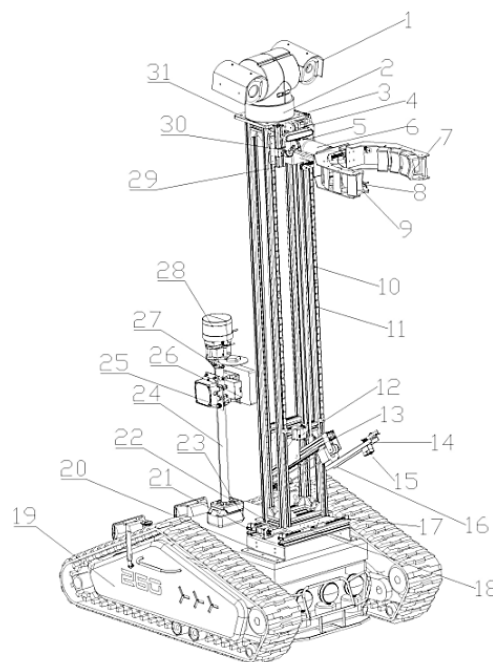


**Fig. 1 - Schematic structure of Sunflower Intelligent Plug-in Tray Dryer**

1. environmental information acquisition device; 2. environmental information acquisition device rotating servo; 3. environmental information acquisition device fixed frame; 4. flower disc gripping device moving frame; 5. flower disc gripping device servo motor; 6. flower disc gripping device tipping servo; 7. flower disc gripping device; 8. flower stalk cutting device servo motor; 9. flower stalk cutting device; 10. flower disc gripping device moving guide and main frame; 11. conveyor; 12. conveyor control motor; 13. stem cutting device fixed frame; 14. stem cutting device; 15. stem cutting device servo motor and distance sensor; 16. stem cutting device telescopic frame; 17. main body fixed frame; 18. frame left-right moving device; 19. crawler chassis; 20. frame left-right moving device fixed frame; 21. frame left-right moving device conveyor; 22. frame left-right moving device servo motor; 23. navigation receiver base; 24. support bar; 25. IMU attitude inertial sensor; 26. RTK receiver; 27. LiDAR fixture; 28. LiDAR; 29. binocular camera fixture; 30. binocular camera movable arm; 31. binocular camera



Fig. 2 - Sunflower Intelligent Insert Tray Dryer test prototype

According to the above design ideas, the sunflower intelligent plug tray drying machine overall structure design shown in Fig.1, is mainly divided into mechanical design part and intelligent equipment part (Young *et al.*, 2019). In the mechanical design part, by simulating the operation process of sunflower tray drying, six parts of grasping, shearing, turning, lifting, telescoping and moving are designed; the tracked chassis is selected and weighted, which fully takes into account the fact that the centre of gravity will be unstable after the completion of the design due to the discs being too high, and also makes it convenient for the agricultural machine to walk on the rugged field ground. In the intelligent equipment section, the integration of environmental information acquisition devices, binocular cameras, LiDAR, and RTK receivers enables the intelligent operation of sunflower planting and drying. The physical prototype is shown in Fig. 2.

### Key Structure and Hardware Selection

#### Design of mechanical structures

This design of sunflower tea tray drying robot contains a flower tray grasping structure, a stem cutting device, a lifting device, a stem cutting device, and a rack moving device (shown in Fig.3). When the binocular camera moves upward, the camera and sensor integration technology recognizes and locates the flower plate (Fang *et al.*, 2018). After the localization is completed, the motor drives the gripper jaws to complete the gripping. In the case of failing to locate the flower disk, the device control system will speculate the position of the disk by recognizing the flower stem direction and some disk features. If the recognition fails, the device will slightly adjust the angle or height of the camera to help the camera better capture the front or side of the disk. After the capture is completed, the controller sends a signal and the motor drives the conveyor belt through gear transmission to realize the structure lifting and lowering. The stem shearing device consists of a fixed part and a moving part, and the motor drives the shearing device to telescope through gears and a conveyor belt. After grasping and turning over, the distance sensor measures the distance of the stem, and the motor controls the shears to complete the shearing. The frame moving device controls the conveyor belt to move on the guide rail through the motor and adjusts the horizontal position of the frame to ensure accurate completion of gripping and shearing. The power drive is driven by stepper motor with lead-acid battery power supply. The stepper motor has excellent positioning accuracy and speed control capability to ensure the accuracy and consistency of the shearing, lifting and inserting operations. Lead-acid batteries have low energy density, but are low cost and durable. A single charge can support continuous operation for about 2-3 hours, which meets the endurance requirements of small-scale field operations. Users can further extend the operating time by replacing the batteries.

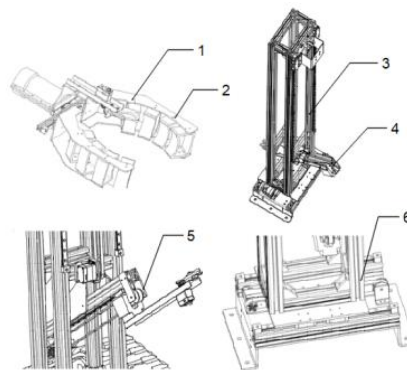
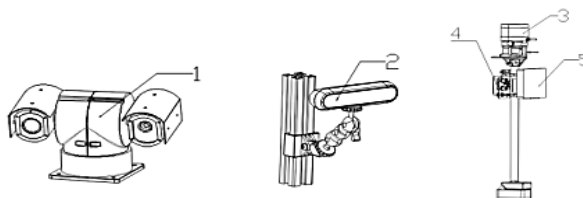


Fig. 3 - Schematic diagram of the mechanical structure of Sunflower Intelligent Insert Tray Dryer

1. stalk shearing device; 2. disc gripping structure; 3. lifting device; 4. stalk shearing device fixing component;
5. stalk shearing device moving component; 6. frame moving device

**Intelligent structural design**

The key structures of the intelligent design include the environmental information acquisition device, binocular camera and LIDAR (shown in Fig.4). The environmental information acquisition device is used to identify and locate sunflowers in the field, together with the LiDAR for distance judgement and equipment attitude adjustment (Shi et al., 2023; Peteinatos et al., 2014). A binocular camera enhances the recognition and localisation capabilities and assists the flower disc grasping structure for accurate grasping (Williams et al., 2019; Zhu et al., 2021). The LiDAR, on the other hand, is responsible for device localisation, helping to build graphics, plan routes, avoid obstacles and navigate (Bechar et al., 2016).



**Fig. 4 - Schematic diagram of intelligent structure of Sunflower Intelligent Insertion Tray Dryer**  
 1. Environmental Information Acquisition Unit (EIAU); 2. Binocular Camera; 3. LiDAR; 4. RTK Receiver; 5. IMU Attitude Sensor

**Software design**

Machine parameters are set through the configured host computer, as shown in Table 1. Set the baud rate in the "serial port settings" interface, open the serial port to receive real-time feedback data from the servo, and confirm that the computer is connected to the servo normally. Servo control module can independently or simultaneously control the servo ID1-7, the default speed of 1000, range 0-32766, angle range 0-32766, enter the servo position, select and click on the operation, the feedback position value will have a ±5 error. The device supports initialisation and one-button neutrality function. At initialisation, all servos move left and right and return to the minimum angle/0 position; one-key neutral function sets the current servo position to 2048 neutral. In servo mode, the servos can perform different position movements. After writing the target position, click to complete the operation. The system currently only supports one write operation, and cannot be executed multiple times. When deleting the content, please delete all the written content at once and reset the servo to the minimum angle/0 position.

**Table 1**

**Servo serial number and control parameters**

| Position                                | Helm number | Parameters and operating range    |
|---|-------------|-----------------------------------|
| Top opening and closing grippers        | ID 1        | 0-2600                            |
| Top rotating gripper                    | ID 2        | 0-1380                            |
| Upper and lower jointed robotic arms    | ID 3        | Upper unit to view servo position |
| Right and left articulated robotic arms | ID 4        | Upper unit to view servo position |
| Upper scissor control joints            | ID 5        | 5-2500                            |
| Lower scissor control joints            | ID 6        | 5-2500                            |
| Forward control joints                  | ID 7        | Upper unit to view servo position |

**Workflow**

After the device enters the field, the environmental information acquisition device starts immediately, collects information about the surrounding environment, and identifies and localizes the sunflower plant through the deep learning algorithm. The LiDAR scans synchronously, plans an obstacle-free route and turns on the obstacle avoidance function, determines the position of the sunflower and the device, and feeds back the movement coordinates to the mobile control mechanism (see Fig.5). As the device approaches the target crop, it stops at a distance of about 10 cm from the sunflower. The gripper jaws begin to rise, and when the binocular camera recognizes the disk, the gripper jaws stop and feed back to the motor, which contracts and completes the fine-tuning to ensure that the disk is grabbed. After the jaws have contracted, the stalk cutter is activated and the motor controls the opening and closing of the scissors to cut the stalks from the disk. Subsequently, the stalk shearing device extends and is positioned by the distance sensor and the fine adjustment mechanism, stopping when the distance is 0. The scissors motor cuts the stalks. Subsequently, the clamping jaws flip to remove the flower disk and descend to the set distance, then the sunflower disk is firmly inserted into the stalks that have just been cut, completing the insertion of the flower disk for drying process. After the clamping jaws are reset, the mobile mechanism backs up, and the information acquisition device re-recognizes the next target and enters the next round of operation.

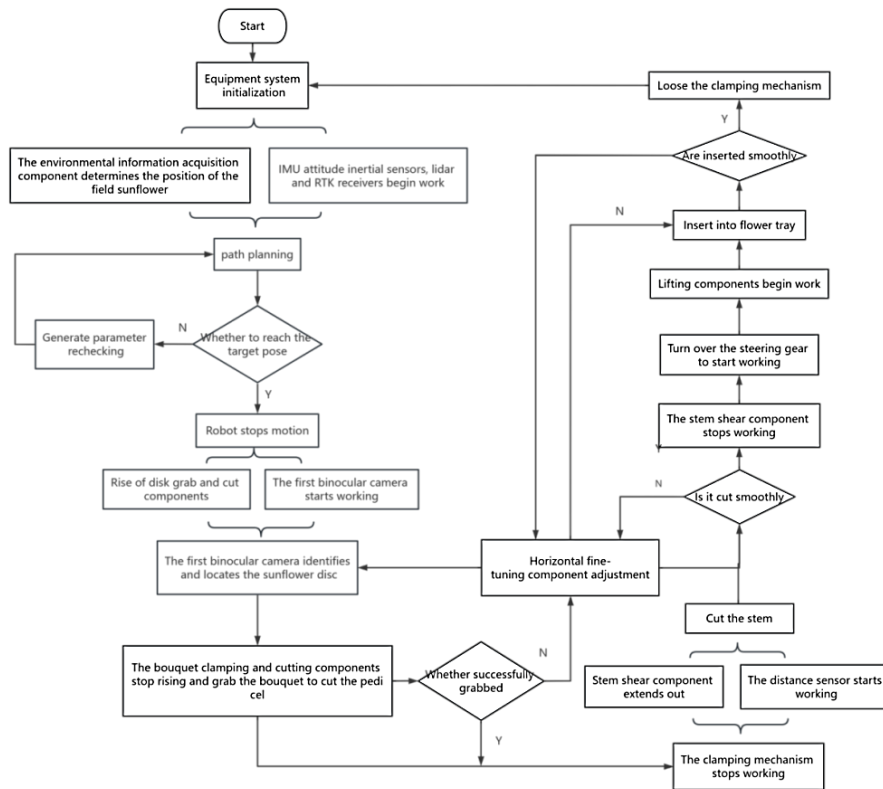


Fig. 5 - Planning of sunflower plug tray drying operation

**Target identification design**

In this study, the lightweight YOLOv5 target detection model was used to identify sunflower discs. The experimental data were obtained from the experimental base of Shanxi Agricultural University and the experimental base of its Economic Crops Research Institute in Wujiabao, Taigu District, Jinzhong City, Shanxi Province. To reduce the influence of light intensity and camera angle on the detection results, 2213 sunflower disc images in different weather, time and angle were taken. Meanwhile, 278 flower disc images were selected from the Kaggle floral public dataset, totalling 5697 images, including data expanded by contrast adjustment, flipping and mirroring. The dataset was annotated using LabelIMG tool and saved as an XML file in Pascal VOC format. The recognition process of sunflower discs is shown in Fig.6.

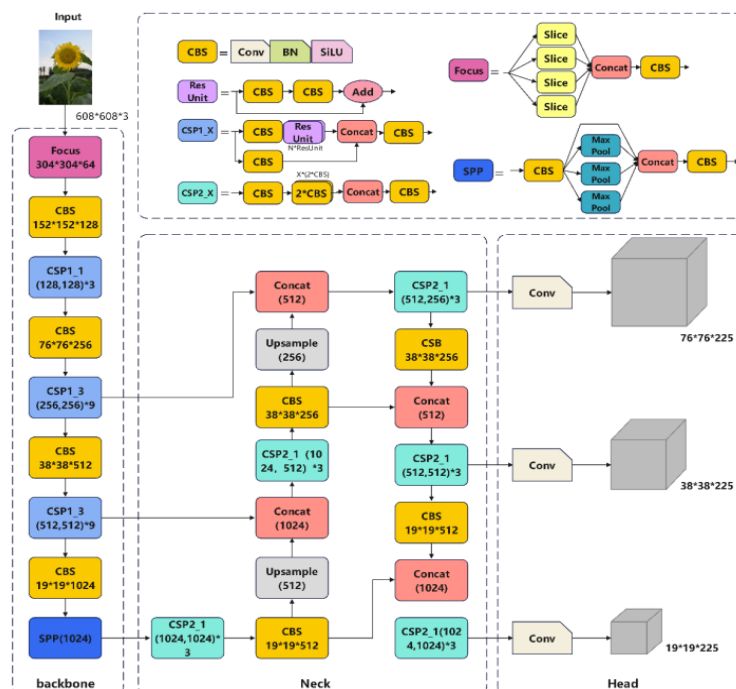


Fig. 6 - YOLOv5 detection model



**Performance indicator**

In order to represent the performance of the model, it was decided to use the Average Precision of the categories (Average Precision), the Mean of Average Precision of the categories (mAP), the F1-score, the number of parameters, and the model's occupied memory as model evaluation metrics. Precision P and Recall R can be defined by the following equations:

$$P = \frac{TP}{TP + FP} \times 100\% \tag{1}$$

$$R = \frac{TP}{TP + FN} \times 100\% \tag{2}$$

Therefore, the category accuracy AP can also be derived:

$$AP = \int_0^1 P(R) dR \tag{3}$$

mAP is the average of the AP values for multiple categories. If there are N categories, mAP can be expressed as:

$$mAP = \frac{1}{N} \cdot \sum_{i=1}^N AP_i \tag{4}$$

F1 is the reconciled average of precision and recall and is often used to evaluate the balance of the model. It is given by the formula:

$$F1 = 2 \times \frac{P \times R}{P + R} \tag{5}$$

**Field path navigation design**

In an agricultural environment, a machine vision-based navigation and positioning system performed well in good lighting conditions, with recognition accuracy of 97.8 percent (sunny) and 85.3 percent (cloudy), but decreased to 56.4 percent at night. Global navigation satellite systems (GNSS) provide real-time position information, but the error increases to ±5 metres in occluded environments. LiDAR becomes a reliable choice due to its high ranging accuracy and anti-interference, with the error controlled within ±0.1 m. Taking it into consideration, a navigation scheme is designed: machine vision is preferred when there is good light; when there are a lot of occlusions, switch to GNSS; rely on LiDAR for precise positioning in areas with low light or complex terrain. Fig.7 shows the path navigation design planning flow chart.

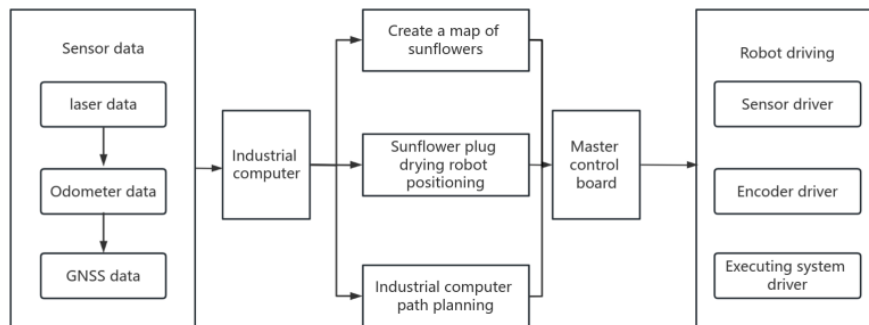


**Fig. 7 - Flowchart of path navigation design**

**Assessment of indicator**

In order to evaluate the performance of the algorithm, it was decided to use Root Mean Square Error (RMSE), Standard Deviation (STD) as the evaluation metrics for the LeGO-LOAM algorithm. The following are the formulas for these two metrics.

$$RMSE = \sqrt{\frac{1}{n} \sum_{i=1}^n (y_i - \hat{y}_i)^2} \tag{6}$$

$$STD = \sqrt{\frac{1}{n-1} \sum_{i=1}^n (x_i - \bar{x}_i)^2} \tag{7}$$

**RESULTS**

**Tests and analyses of insert tray drying operations**

To verify the feasibility of the plug tray drying experiment, 81 samples of drying sunflower plants were collected for destructive sampling and their disc diameter, plant height, stem diameter and stalk diameter were measured. Because the dryer design needs to take into account different plant heights, a wide range of plant heights was designed, ranging from 60 cm to 200 cm. Stable data on stem and peduncle diameters were concentrated in the range of 2 to 3 cm and less than 1 cm, respectively, which facilitated the design of mechanical clamping or shearing devices. Flower disc diameters were predominantly in the 20 cm range, influencing the design of mechanical devices to accommodate different disc sizes. Based on the data calculations, the final prototype design parameters included a base 106 cm long, 80 cm wide, and 204.5 cm high; a gripping jaw range of 18 to 36 cm and a lifting range of 98 to 196.5 cm; and a shear device with a maximum retractable distance of 31 cm and an opening and closing distance of 6 cm. These parameters ensure that the prototype is capable of efficiently and automatically executing sunflower plug tray drying operations. It has been experimentally verified that the processing time of a single disk is about 10 seconds, and about 330 disks can be processed in one hour. However, the specific area covered by the operation is subject to change according to the planting density.

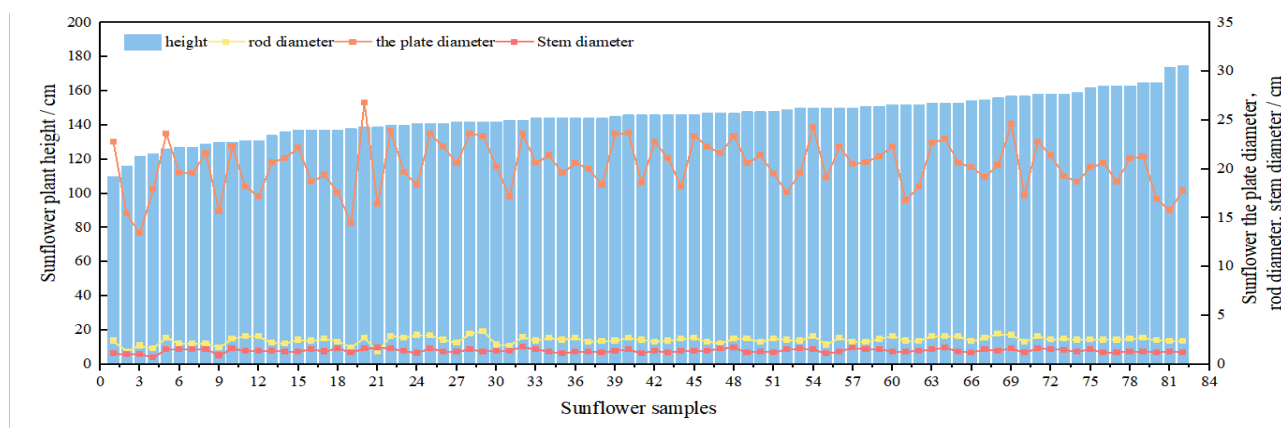


**Fig. 8 - Sunflower sample data collection map**

Plate drying test is the operator to operate the machine through the clamping claw assembly to grasp the flower plate and cut (a), flip the structure to control the clamping claw flip (b), the stem shear assembly to cut the flower stalk (c), left and right fine-tuning structure to move 5cm and with the lifting assembly to complete the lifting and moving the insertion of sunflower plate (d), and ultimately to achieve the drying of the flower plate. Due to precision limitations, each component's servo motor movement is subject to an error of  $\pm 5$ . After several adjustments to the position of each component, the basic motion parameter range of the servo was determined, greatly expanding the operational space for disc insertion and ensuring the successful completion of the task. The prototype test results are shown in Fig. 9.

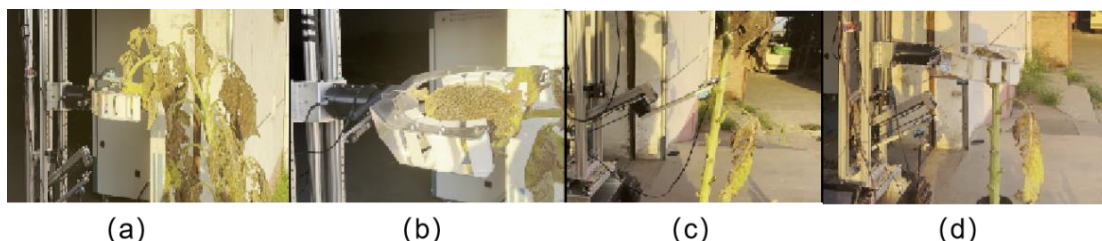


**Fig. 9 - Sunflower plug tray drying test plot**

**Analysis of sunflower identification detection results**

Experimental validation shows that the YOLOv5 model performs well in the sunflower disc recognition task. The overall category accuracy reached 95.54%, precision was 89.94%, recall was 95.54%, and F1 value was 0.89 (Fig.10).

In the different orientation tests, the category precision of the model in the frontal, side, top, and back orientations were 96.00%, 95.00%, 95.50%, and 95.00%, respectively; the precision in all orientations exceeded 90.00%, and the recall rate exceeded 95.00%, as shown in Table 1. In the comprehensive evaluation, the highest F1 value was 0.92 for the frontal direction, and the rest of the directions remained at 0.91 (Fig.11). The results show that the YOLOv5 model not only has excellent overall recognition performance, but also has excellent robustness and efficiency in multi-direction tests.



Fig.10 - Sunflower recognition results

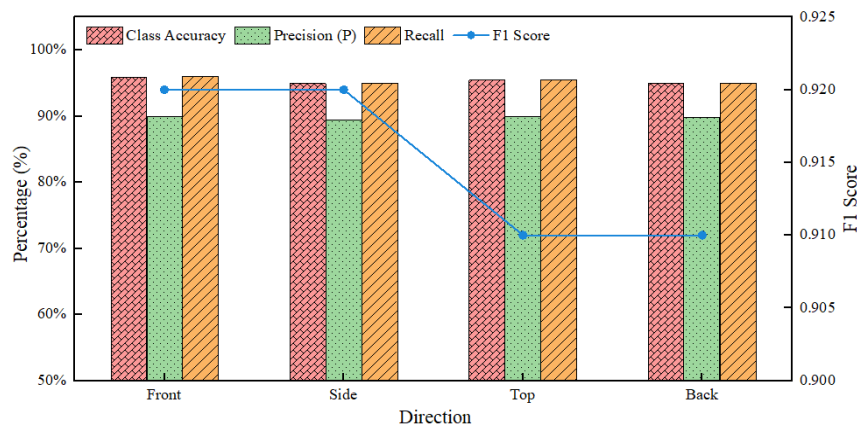


Fig. 11 - Multi-directional test results

Table 2

| Multi-directional recognition test results |                |               |         |          |
|--|----------------|---------------|---------|----------|
| Direction                                  | Class Accuracy | Precision (P) | Recall  | F1 Score |
| Front                                      | 96.00 %        | 90.00 %       | 96.00 % | 0.92     |
| Side                                       | 95.00 %        | 89.50 %       | 95.00 % | 0.92     |
| Top  | 95.50 %        | 89.90 %       | 95.50 % | 0.91     |
| Back                                       | 95.00 %        | 89.80 %       | 95.00 % | 0.91     |

**Navigational mapping test analysis**

The methodology for constructing a map of the sunflower environment includes point cloud scanning and processing, SLAM loopback detection, point cloud alignment and graphical optimisation (Almazrouei et al., 2023). In this study, 16-line 3D LiDAR is used on a tracked mobile chassis for point cloud data acquisition at a speed of 0.5-1 m/s and a frequency of 10 Hz. The map is constructed using the LeGO-LOAM algorithm, and the experimental results show that the root-mean-square error (RMSE) of the trajectory is 0.15 m, with a standard deviation of 0.10 m. The purple line is the preset trajectory and the green line is the actual trajectory, and the purple line is the preset trajectory and the green line is the actual trajectory, which are highly consistent, but the green line in the turning area is slightly deviated, indicating that the error is mainly concentrated in the turning adjustment. The figure on the right represents the absolute position error of the trajectory in the spatial coordinate system, and the closer the colour is to red, the greater the error, which is consistent with the navigation trajectory diagram in the left figure.



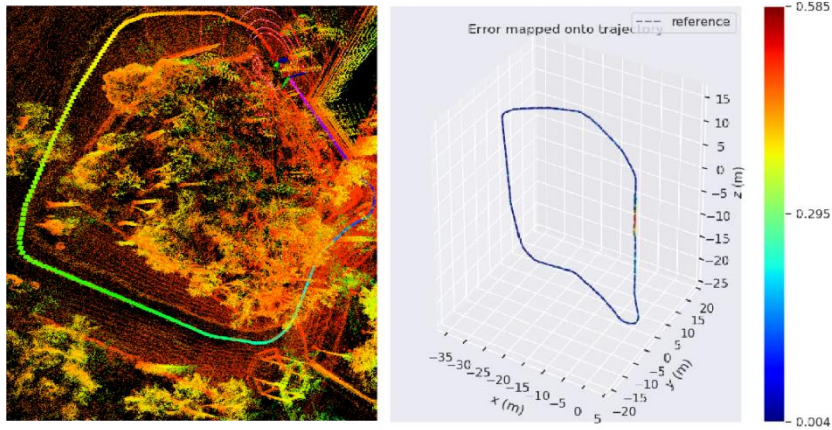


Fig. 12 - Graph of building test results

In this experiment, the path error of the robot was measured several times while navigating through a field of sunflowers. Table 2 lists the scheduled path length, actual path length, path deviation rate, error mean and error standard deviation data for the five sets of tests. Fig.12 demonstrates the trend of error with path length. The results show that when the predetermined path length is 100 metres, the error mean is 0.15 metres and the standard deviation is 0.10 metres; when the path length increases to 300 metres, the error mean is 0.17 metres and the standard deviation is 0.12 metres. Although the increase in path length resulted in a slight increase in error, the overall error remained low. The path deviation rates for all tests ranged from 0.20% to 0.26%, indicating that the actual path of the robot deviated very little from the intended trajectory. The algorithm performs stably in sunflower field navigation and meets the needs of sunflower insertion tray drying and autonomous navigation.

Table 3

Robot navigation test data

| Test Number                  | 1     | 2     | 3     | 4     | 5     |
|------------------------------|-------|-------|-------|-------|-------|
| Planned Path Length (m)      | 100   | 150   | 200   | 250   | 300   |
| Actual Path Length (m)       | 100.2 | 150.3 | 300.4 | 250.6 | 300.8 |
| Path Deviation Rate (%)      | 0.2   | 0.2   | 0.2   | 0.24  | 0.26  |
| Mean Error (m)               | 0.15  | 0.14  | 0.16  | 0.15  | 0.17  |
| Error Standard Deviation (m) | 0.1   | 0.11  | 0.09  | 0.1   | 0.12  |

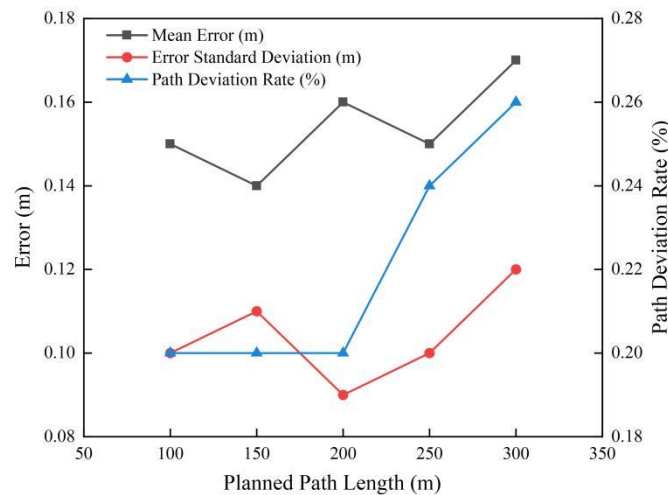


Fig. 13 - Path error analysis diagram

**CONCLUSIONS**

In this paper, an intelligent sunflower insertion tray drying machine is proposed, which has the functions of intelligent recognition of sunflower trays and navigation and map building, and significantly improves the work efficiency. Field experiments comprehensively verified the performance of the device.

The experimental results show that the category accuracy of the YOLOv5 model in the multi-direction test of the flower discs exceeds 95%, demonstrating good recognition stability and robustness.

The navigation building tests using the LeGO-LOAM algorithm show that the robot's path tracking error is small, with path deviation rates ranging from 0.20% to 0.26%. However, in the tests with different path lengths, the error in the turning area was large, reaching 0.3 m to 0.585 m. The turning mechanism needs to be optimised to reduce the error. The error of navigation building is mainly concentrated in the complex terrain area, and the point cloud processing algorithm should be optimised to improve the positioning accuracy.

In addition, it was found that the diameter of the flower discs was concentrated around 20 cm, which accounted for 85% of the total samples, and a more flexible jaw structure needs to be designed to increase the clamping range. In the future, the processing speed and range can be further optimized to adapt to the needs of larger-scale operations, which provides a proven solution for agricultural mechanization.

## ACKNOWLEDGEMENT

This project was funded by the Construction Project of Modern Agricultural Industrial Technology System of Shanxi Province (2023CYJSTX05-17), the Key Research and Development Programme of Shanxi Province (202202140601021) and the Sub-theme of the National Key Research and Development Programme (2021YFD1600301-4).

## REFERENCES

- [1] Jin, Y., Liu, J., Xu, Z., Yuan, S., Li, P. and Wang, J., 2021. Development status and trend of agricultural robot technology. *International Journal of Agricultural and Biological Engineering*, 14(4), pp.1-19.
- [2] Dhanaraju, M., Chenniappan, P., Ramalingam, K., Pazhanivelan, S. and Kaliaperumal, R., 2022. Smart farming: Internet of Things (IoT)-based sustainable agriculture. *Agriculture*, 12(10), p.1745.
- [3] Peng, J., Zhao, Z. and Liu, D., 2022. Impact of agricultural mechanization on agricultural production, income, and mechanism: evidence from Hubei province, China. *Frontiers in Environmental Science*, 10, p.838686.
- [4] Moschen, S., Gialdi, A.I.L., Paniego, N., Fernandez, P. and Heinz, R.A., 2017. Sunflower leaf senescence: a complex genetic process with economic impact on crop production. In *Senescence-Physiology or Pathology*. IntechOpen.
- [5] Pan, F., Chen, J., Zhang, H., Han, L., Dong, Y., Li, B. and Ji, C., 2024. Design and Experiment of Plate Taking Control System of Edible Sunflower (*Edulis Helianthus Catino L.*) Harvester. *Agriculture*, 14(4), p.592.
- [6] Dong, S., Yuan, Z., Gu, C., Yang, F., Fu, H., Wang, C., Jin, C. and Yu, J., 2017. Research on intelligent agricultural machinery control platform based on multi-discipline technology integration. *Transactions of the Chinese Society of Agricultural Engineering*, 33(8), pp.1-11.
- [7] Li, C.E., Tang, Y., Zou, X., Zhang, P., Lin, J., Lian, G. and Pan, Y., 2022. A novel agricultural machinery intelligent design system based on integrating image processing and knowledge reasoning. *Applied Sciences*, 12(15), p.7900.
- [8] Young, S.N., Kayacan, E. and Peschel, J.M., 2019. Design and field evaluation of a ground robot for high-throughput phenotyping of energy sorghum. *Precision Agriculture*, 20(4), pp.697-722.
- [9] Fang, B., Sun, F., Yang, C., Xue, H., Chen, W., Zhang, C., Guo, D. and Liu, H., 2018, May. A dual-modal vision-based tactile sensor for robotic hand grasping. In *2018 IEEE International Conference on Robotics and Automation (ICRA)* (pp. 4740-4745). IEEE.
- [10] Shi, J., Bai, Y., Diao, Z., Zhou, J., Yao, X. and Zhang, B., 2023. Row detection BASED navigation and guidance for agricultural robots and autonomous vehicles in row-crop fields: methods and applications. *Agronomy*, 13(7), p.1780.
- [11] Peteinatos, G.G., Weis, M., Andújar, D., Rueda Ayala, V. and Gerhards, R., 2014. Potential use of ground-based sensor technologies for weed detection. *Pest management science*, 70(2), pp.190-199.
- [12] Williams, H.A., Jones, M.H., Nejati, M., Seabright, M.J., Bell, J., Penhall, N.D., Barnett, J.J., Duke, M.D., Scarfe, A.J., Ahn, H.S. and Lim, J., 2019. Robotic kiwifruit harvesting using machine vision, convolutional neural networks, and robotic arms. *Biosystems Engineering*, 181, pp.140-156.
- [13] Zhu, K. and Zhang, T., 2021. Deep reinforcement learning based mobile robot navigation: A review. *Tsinghua Science and Technology*, 26(5), pp.674-691.
- [14] Bechar, A. and Vigneault, C., 2016. Agricultural robots for field operations: Concepts and components. *Biosystems Engineering*, 149, pp.94-111.
- [15] Almazrouei, K., Kamel, I. and Rabie, T., 2023. Dynamic obstacle avoidance and path planning through reinforcement learning. *Applied Sciences*, 13(14), p.8174.